Inorg. Chem. **2007**, *46*, 117−124

A Density Functional Theory Study of the Electronic Properties of Os(II) and Os(III) Complexes Immobilized on Au(111)

Noel M. O'Boyle,*,†,‖ Tim Albrecht,‡,⊥ Daniel H. Murgida,§ Lynda Cassidy,† Jens Ulstrup,‡ and Johannes G. Vos*,†

National Centre for Sensor Research, School of Chemical Sciences, Dublin City University, Glasnevin, Dublin 9, Ireland, Department of Chemistry, Technical University of Denmark, Dk-2800 Lyngby, Denmark, Max-Volmer-Laboratorium für Biophysikalische Chemie, Institut für Chemie, Technische Universität Berlin, Sekr. PC14, Strasse des 17 Juni 135, D-10623 Berlin, Germany

Received May 24, 2006

We present a density functional theory (DFT) study of an osmium polypyridyl complex adsorbed on Au(111). The osmium polypyridyl complex $[Os(bpy)_2(P0P)Cl]^{n+}$ [bpy is 2,2′-bipyridine, P0P is 4,4′-bipyridine, $n = 1$ for osmium(II), and $n = 2$ for osmium(III)] is bound to the surface through the free nitrogen of the P0P ligand. The calculations illuminate electronic properties relevant to recent comprehensive characterization of this class of osmium complexes by electrochemistry and electrochemical scanning tunneling microscopy. The optimized structures for the compounds are in close agreement with crystallographic structures reported in the literature. Oxidation of the complex has little effect on these structural features, but there is a substantial reordering of the electronic energy levels with corresponding changes in the electron density. Significantly, the highest occupied molecular orbital shifts from the metal center to the P0P ligand. The surface is modeled by a cluster of 28 gold atoms and gives a good description of the effect of immobilization on the electronic properties of the complexes. The results show that the coupling between the immobilized complex and the gold surface involves electronic polarization at the adsorbate/substrate interface rather than the formation of a covalent bond. However, the cluster is too small to fully represent bulk gold with the result that, contrary to what is experimentally observed, the DFT calculation predicts that the gold surface is more easily oxidized than the osmium(II) complex.

Introduction

The miniaturization of electronic components has enabled the semiconductor industry to produce smaller, faster, and more efficient components year after year. However, as existing "top-down" technologies for construction of electronic circuits have approached a limit where quantum effects start to interfere, there has been increasing interest in "bottom-up" approaches, the area of molecular electronics. This involves control of the charge transfer at the nanoscale level[1] by using single or small groups of molecules as components in electronic devices, an idea first introduced by Aviram and Ratner in 1974.[2] Systems involving redox-active molecules attached to a substrate surface are of particular interest because they may act as molecular transistors.[3−5] Recent scanning tunneling microscopy (STM) studies of the complex $[Os(bpy)_2(P0P)Cl]^+$, where P0P is 4,4′-bipyridine and bpy is 2,2′-bipyridine (Figure 1) revealed *room temperature* transistor-like properties for this compound

* To whom correspondence should be addressed. E-mail: han.vos@dcu.ie (J.G.V.), noel.oboyle2@mail.dcu.ie (N.M.O'B.). Tel: +35317005307 (J.G.V.). Fax: +35317005503 (J.G.V.).

† Dublin City University.

‖ Current address: Unilever Centre for Molecular Science Informatics, Department of Chemistry, University of Cambridge, Lensfield Road, Cambridge CB2 1EW, U.K.

‡ Technical University of Denmark.

⊥ Present address: Theoretical and Experimental Physical Chemistry Section, Department of Chemistry, Imperial College London, South Kensington Campus, London SW7 2AZ, U.K.

§ Technische Universität Berlin.

(1) Adams, D. M.; Brus, L.; Chidsey, C. E. D.; Creager, S.; Creutz, C.; Kagan, C. R.; Kamat, P. V.; Lieberman, M.; Lindsay, S.; Marcus, R. A.; Metzger, R. M.; Michel-Beyerle, M. E.; Miller, J. R.; Newton, M. D.; Rolison, D. R.; Sankey, O.; Schanze, K. S.; Yardley, J.; Zhu, X. *J. Phys. Chem. B* **2003**, *107*, 6668−6697.

(2) Aviram, A.; Ratner, M. A. *Chem. Phys. Lett.* **1974**, *29*, 277−283.

(3) Kuznetsov, A. M.; Ulstrup, J. *J. Phys. Chem. A* **2000**, *104*, 11531−11540.

(4) Kuznetsov, A. M.; Ulstrup, J. *Electrochim. Acta* **2000**, *45*, 2339−2361.

(5) Zhang, J.; Kuznetsov, A. M.; Ulstrup, J. *J. Electroanal. Chem.* **2003**, *541*, 133−146.

10.1021/ic060903e CCC: $37.00
Published on Web 12/07/2006

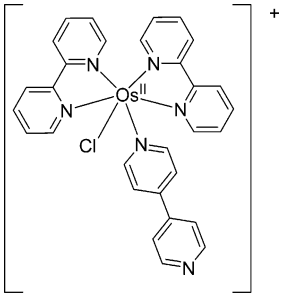

OsP0P

Figure 1. Structure of **OsP0P**, $[Os(bpy)_2(P0P)Cl]^+$.

when immobilized on platinum or gold surfaces.[6] Ulstrup and Kuznetsov[3−5] have developed a comprehensive electron-transfer theory to explain the characteristics of tunneling in such a three-level system: STM tip Fermi level, molecular redox potential, and surface Fermi level. The results obtained for osmium complexes of the type outlined above indicate that the osmium(II/III) redox couple indeed mediates electron tunneling between the STM tip and the surface.

The tunneling behavior observed depends strongly on the coupling between the molecular states of the metal complex and those of the substrate. In addition, this coupling may depend on the redox state of the surface-bound species. With this in mind, the present contribution describes a density functional theory (DFT)-based computational study of the electronic properties of $[Os(bpy)_2(P0P)Cl]^+$ (**OsP0P**) and its oxidized form, $[Os(bpy)_2(P0P)Cl]^{2+}$ (**OsP0Pox**). The focus of the study is the computational description of the nature of the molecular energy levels and the electron density in both oxidation states, both in the free state and when adsorbed on gold.

Computational Methods

All calculations were carried out using *Gaussian03*[7] and the hybrid DFT functional B3LYP.[8−11] The LanL2DZ basis set and electron core potential (ECP) of Dunning, Hay, and Wadt were used for all atoms of the osmium complexes. For the atoms carbon, hydrogen, and nitrogen, LanL2DZ uses the Dunning/Huzinaga valence double-ζ basis set.[12] For osmium, LanL2DZ uses an ECP for the innermost 60 electrons. The remaining 16 electrons were treated using a double-ζ basis set.[13] The structures of the complex **OsP0P** and its oxidized analogue **OsP0Pox** were optimized at the B3LYP/LanL2DZ level of theory. A restricted DFT calculation was carried out on **OsP0P**, which has an even number of electrons.

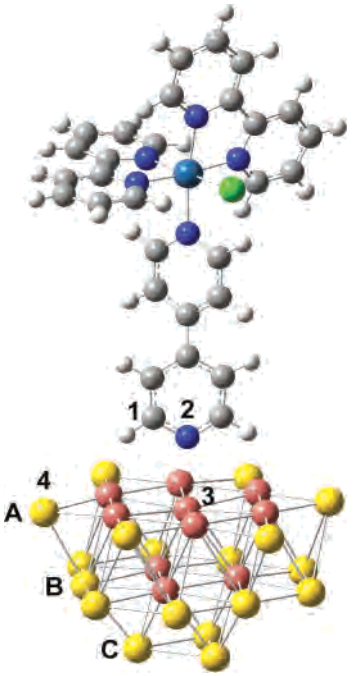

Figure 2. Optimized structure of **OsP0P** adsorbed on the surface of the gold cluster. The numbers indicate atoms referred to in the text. The letters indicate the three layers of the gold cluster. In our analysis, a larger basis set (LanL2DZ) was used for the valence electrons of the central atom of layer A and its neighboring atoms (colored pink). For the other gold atoms (colored yellow), the smaller LanL2MB basis set was used.

Because of the odd number of electrons in the oxidized species, an unrestricted calculation was required for **OsP0Pox**. Frequency calculations were carried out on the optimized geometry at the same level of theory. The instantaneous change in the electron density upon oxidation was calculated by performing a single-point energy calculation at the optimized geometry of **OsP0P** with a charge of 2+ and a multiplicity of 2. The resulting total density was subtracted from that of **OsP0P** using the cubman utility of *Gaussian03*.

A cluster model of 28 gold atoms was used for the gold surface, which consisted of three layers of 13, 12, and 3 atoms (labeled A, B, and C, respectively, in Figure 2). The LanL2DZ pseudopotential and basis set was used for the central atom of the first layer and its nine immediate neighbors (colored pink in Figure 2). The LanL2MB pseudopotential and basis set was used for the remaining gold atoms (colored yellow in Figure 2). The LanL2MB basis set uses the same size ECP as the LanL2DZ basis set (in each case, it accounts for the innermost 60 electrons), but a minimal basis set is used for the remaining 19 valence electrons. The geometry of the cluster was optimized under C_{3v} symmetry from an initial geometry equivalent to the bulk structure of gold.

To study the adsorption of the osmium complexes on gold, each osmium complex was placed on the surface such that the long axis of the P0P ligand was perpendicular to layer C of the gold cluster and the free nitrogen of the P0P ligand was directly over the central gold atom of layer A. The geometry of the adsorbed complex was optimized with 2 degrees of freedom: the distance between the complex and the surface (the distance from 2 to 3 in Figure 2) and the dihedral angle between the P0P ligand and two gold atoms on the surface (the dihedral angle formed by 1−2−3−4 in Figure 2). As for the isolated complex, restricted calculations were performed for Au_{28}/**OsP0P** and unrestricted calculations for Au_{28}/**OsP0Pox**.

GaussSum[14] was used to calculate the fractional contributions of various groups to each molecular orbital. This is done using Mulliken population analysis. *GaussSum* was also used to convolute

(6) (a) Albrecht, T.; Guckian, A.; Ulstrup, J.; Vos, J. G. *Nano Lett.* **2005**, *5*, 1451−1455. (b) Albrecht, T.; Guckian, A.; Ulstrup, J.; Vos, J. G. *IEEE Trans. Nanotechnol.* **2005**, *4*, 430−434. (c) Albrecht, T.; Moth-Poulsen, K.; Christensen, J. B.; Guckian, A.; Bjornholm, T.; Vos, J. G.; Ulstrup, J. *Faraday Discuss.* **2006**, *131*, 265−279.
(7) Frisch, M. J.; Trucks, G. W.; Schlegel, H. B.; et al. *Gaussian03*, revision B.04; Gaussian, Inc.: Wallingford, CT, 2004.
(8) Becke, A. D. *J. Chem. Phys.* **1993**, *98*, 5648−5652.
(9) Lee, C.; Yang, W.; Parr, R. G. *Phys. Rev. B* **1988**, *37*, 785−789.
(10) Miehlich, B.; Savin, A.; Stoll, H.; Preuss, H. *Chem. Phys. Lett.* **1989**, *157*, 200−206.
(11) Stephens, P. J.; Devlin, F. J.; Chabalowski, C. F.; Frisch, M. J. *J. Phys. Chem.* **1994**, *98*, 11623−11627.
(12) Dunning, T. H., Jr.; Hay, P. J. In *Modern Theoretical Chemistry*; Schaefer, H. F., III, Ed.; Plenum: New York, 1976; Vol. 3, pp 1−28.
(13) (a) Hay, P. J.; Wadt, W. R. *J. Chem. Phys.* **1985**, *82*, 270−283. (b) Wadt, W. R.; Hay, P. J. *J. Chem. Phys.* **1985**, *82*, 284−298. (c) Hay, P. J.; Wadt, W. R. *J. Chem. Phys.* **1985**, *82*, 299−310.

Table 1. Selected Geometrical Properties of the Osmium Complexes Studied[a]

	crystal **OsP0P**[b]	**OsP0P**	**OsP0Pox**
Os−Cl	2.42	2.50	2.43
Os−N_{P0P}	2.10	2.12	2.14
Os−N_{bpy1} (trans to P0P)	2.05	2.06	2.09
Os−N_{bpy1}	2.06	2.07	2.09
Os−N_{bpy2} (trans to Cl)	2.02	2.07	2.10
Os−N_{bpy2}	2.06	2.04	2.08
py−py_{P0P} dihedral (deg)	24	29	27

[a] All distances are in angstroms. [b] Crystal structure of $[Os(bpy)_2(P0P)Cl](BF_4)$, from Ryabov et al.[15]

a density of states spectrum from the molecular orbital data for Au_{28}, using Gaussian curves with a full width at half-maximum of 0.1 eV.

Experimental Methods

Resonance Raman spectra were measured from CH_3CN solutions placed in a cylindrical quartz cuvette that was rotated at ca. 20 Hz to avoid laser-induced degradation. The 514-nm line of an argon ion laser (Coherent Innova 70C) was focused on the sample by means of a long working distance objective (20×; NA = 0.35; WD = 2 cm) and adjusted to 1 mW. The scattered light was collected in backscattering geometry using a confocal microscope coupled to a single-stage spectrograph (Jobin Yvon XY) equipped with a 1800 line mm^{-1} grating and a liquid-nitrogen-cooled back-illuminated CCD detector. Elastic scattering and reflected light were rejected with a supernotch filter (Kaiser). The band-pass was set to 2.5 cm^{-1}, and the acquisition time was 2 min. Fourier transform infrared (FT-IR) experiments were recorded on a KBr disk using a Perkin-Elmer 2000 GX FT-IR spectrometer with a resolution of 2 cm^{-1} at a rate of 20 scans min^{-1} in the range 4000−400 cm^{-1}.

Results and Discussion

Osmium Complexes. (a) Structural Features. The structures of **OsP0P** and **OsP0Pox** were optimized at the B3LYP/LanL2DZ level of theory. Table 1 shows the metal-to-ligand distances in the optimized structures. These values are compared to the corresponding values taken from the crystal structure of **OsP0P**, $[Os(bpy)_2(P0P)Cl](BF_4)$, obtained by Ryabov et al.[15] Three of the Os−N_{bpy} distances agree to within 0.01 Å, while the Os−N_{P0P} distances differ by only 0.02 Å. However, in the crystal structure, the Os−N_{bpy} bond length trans to the chlorine atom is considerably shorter at 2.02 Å because of a lack of competition for the back-bonding dπ orbitals of osmium.[16] The calculated structure of **OsP0P** does not show this effect, and the corresponding bond length is 2.07 Å. The Os−Cl distance is predicted to be somewhat longer than in the crystal structure (2.50 vs 2.42 Å). Although the P0P pyridine−pyridine dihedral angle is predicted to be slightly larger than that in the crystal structure (29° vs 24°), rotation in the P0P ligand is not expected to be strongly hindered and is most likely sensitive to crystal packing forces.

Table 2. Comparison of Experimental and Calculated Vibrational Frequencies for **OsP0P**

frequency (cm^{-1})	activity[a]	calculated[b] (cm^{-1})
668	IR	664
763	IR	759
842	IR	832
1018	IR	1008
1020	Raman	1026
1321	Raman	1331
1421	IR	1429
1458	IR	1462
1482	Raman	1487
1606	Raman	1606

[a] Raman peaks are taken from resonance Raman measurements in MeCN. IR spectra were measured on KBr disks. [b] Calculated harmonic frequencies are scaled using a scaling factor of 0.975.

Indeed, dihedral angles of 20° (Hesek et al.[17]) and 8° (Du et al.[18]) are found for two crystal structures of the ruthenium analogue of **OsP0P**, $[Ru(bpy)_2(P0P)Cl](PF_6)\cdot H_2O$. Overall, the B3LYP/LanL2DZ level of theory gives results in good agreement with the experimental results.

A comparison of the calculated structures of **OsP0P** and **OsP0Pox** shows that oxidation has little effect on the geometry of the complex because the Os−N bond length increases by only a small amount (0.03 Å on average). This is in agreement with an analysis by Eggleston et al.[16] of the crystal structures of a related ruthenium polypyridyl complex, $[Ru(bpy)_2(Cl)_2]^{n+}$, in the ruthenium(II) and ruthenium(III) states (with $n = 0$ and 1, respectively). On going from the ruthenium(II) state to the ruthenium(III) state, they found that the Ru−N bond length increased on average by 0.02 Å. On the other hand, they found that the Ru−Cl bond length decreased by 0.10 Å upon oxidation. Our data are in good agreement: the calculated Os−Cl bond length decreases by 0.07 Å upon oxidation. Because there is little change in the geometry, the intramolecular reorganization energy in electron transfer is expected to be small. This is in line with the results of electrochemical experiments of Forster for similar osmium complexes,[19] as well as crystallographic data for other ruthenium and osmium complexes.[20−22]

To investigate how well the B3LYP functional describes the potential energy surface around the energetic minimum, experimentally determined vibrational frequencies were compared with the calculated vibrational frequencies (Table 2). The calculated harmonic frequencies were scaled by a constant scaling factor of 0.975, which empirically adjusts for the anharmonicity of the vibrations. Good agreement is found across a broad range of frequencies, which indicates that the level of theory employed is sufficient for our study.

(b) Electronic Properties. Isosurfaces depicting the highest occupied molecular orbital (HOMO) and lowest

(14) O'Boyle, N. M.; Vos, J. G. *GaussSum 1.0*; Dublin City University: Dublin, Ireland, 2005. Available from http://gausssum.sourceforge.net.
(15) Ryabov, A. D.; Roznyatovskaya, N. V.; Suwinska, K.; Revenco, M.; Ershov, A. Y. *J. Biol. Inorg. Chem.* **2003**, *8*, 815−822.
(16) Eggleston, D. S.; Goldsby, K. A.; Hodgson, D. J.; Meyer, T. J. *Inorg. Chem.* **1985**, *24*, 4573−4580.
(17) Hesek, D.; Hembury, G. A.; Drew, M. G. B.; Taniguchi, S.; Inoue, Y. *Inorg. Chem.* **2001**, *40*, 2478−2479.
(18) Du, M.; Ge, X.-J.; Liu, H.; Bu, X.-H. *J. Mol. Struct.* **2002**, *610*, 207−213.
(19) Forster, R. J. *Inorg. Chem.* **1996**, *35*, 3394−3403.
(20) Goodwin, H. A.; Kepert, D. L.; Patrick, J. M.; Skelton, B. W.; White, A. H. *Aust. J. Chem.* **1984**, *37*, 1817−1824.
(21) Fergusson, J. E.; Love, J. L.; Robinson, W. T. *Inorg. Chem.* **1972**, *11*, 1662−1666.
(22) Rillema, D. P.; Jones, D. S.; Levy, H. A. *J. Chem. Soc., Chem. Commun.* **1979**, 849−851.

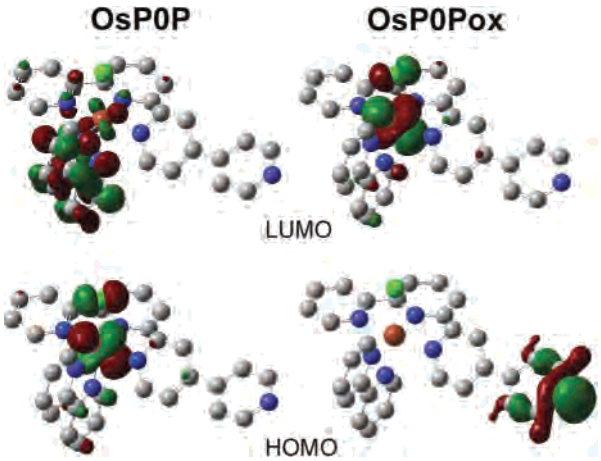

Figure 3. HOMOs and LUMOs of **OsP0P** and **OsP0Pox**. Isosurfaces drawn at 0.04 e bohr^{-3}. Hydrogen atoms are not shown for clarity. Osmium is represented by an orange atom, chlorine by green, nitrogen by blue, and carbon by gray.

unoccupied molecular orbital (LUMO) of **OsP0P** and **OsP0Pox** are shown in Figure 3. The HOMO of **OsP0P** is mainly based on the metal center (66%) and also on the chloride anion, while the LUMO is based on one of the bpy groups. This is in agreement with electrochemical results obtained for **OsP0P**,[6a,23] which show that the oxidation potential is metal-based, while reduction is bpy-based, as is the case for a broad range of osmium polypyridyl complexes.[24] This indicates that the lowest energy transition in **OsP0P** is largely metal-to-ligand charge transfer (MLCT) in character.[23] The calculated electronic structure of the frontier orbitals of **OsP0P** is also in agreement with DFT calculations on the related osmium complex $[Os(bpy)_2(NCS)_2]$ by Guillemoles et al.,[25] who observed that the HOMOs were largely metal-based but with significant contributions from the NCS^- ligands while the LUMO was essentially localized on the bpy groups.

As a first approximation, oxidation could be expected to remove an electron from the HOMO of **OsP0P**, so that the LUMO of **OsP0Pox** is similar to the original HOMO and the new HOMO is either the singly occupied original HOMO or the original HOMO−1. A comparison of the representations of the HOMOs and LUMOs in Figure 3 shows that this simple view has some merit. The LUMO of the oxidized species **OsP0Pox**, based on the metal center with a small contribution from the chloride anion, appears to be identical with the HOMO of **OsP0P**.

To investigate this question further, a Mulliken population analysis was carried out for both complexes using *GaussSum*[14] to describe the molecular orbitals in terms of contributions from the osmium center, the P0P ligand, and the two bpy groups. The results are listed in Tables S1 and S2 in the Supporting Information, and they are visualized in Figure 4. Upon oxidation of **OsP0P**, the molecular orbitals shift to lower energy by about 3 eV (based on a comparison of the corresponding bpy orbitals) due to the increased difficulty of removing an electron. By a comparison of the contributions of the various moieties, it is clear that the LUMO of **OsP0Pox** (% Os/P0P/Cl/bpy is 69:5:10:17) is spatially very similar to the HOMO of **OsP0P** (66:5:14:15). In addition, the LUMO+1 to LUMO+4 of **OsP0Pox** (approximately 5:1:0:94) are similar to the LUMO and LUMO+1 of **OsP0P** (approximately 8:5:1:86) and are bpy-based. However, our simple picture breaks down when we look at the HOMO of the oxidized complex. Somewhat surprisingly, the **OsP0Pox** HOMO is based completely on the P0P ligand (indicated by the red line in Figure 4 at −10.83 eV) and is quite unlike the HOMO−1 of **OsP0P** (approximately 61:3:16:20), contrary to our simple picture of oxidation. In fact, the HOMO of the oxidized species is much more similar to the HOMO−3 of **OsP0P**, which is also represented by a red line in Figure 4 (at −8.82 eV), indicating that it is completely based on the P0P ligand.

These results show that a substantial rearrangement of the occupied orbitals has occurred upon oxidation, so much so that the nature of the lowest energy transition has changed. For **OsP0P**, the lowest energy transition is a MLCT from the osmium center to the bpy ligands. After losing an electron, the lowest energy transition is from the P0P ligand (the new HOMO) to the metal-based LUMO; that is, it is ligand-to-metal charge transfer (LMCT) in character. This agrees with experimental results on osmium(III) polypyridyl complexes, where the lowest energy transition is typically a LMCT.[26] These results mean that the simple picture of an oxidation process painted above is not valid for osmium polypyridyl complexes such as **OsP0P**, although it may have some use in predicting the location of the LUMO in the oxidized species.

An overview of the effect of oxidation on the electron density can be obtained by visualizing the instantaneous change in the electron density upon oxidation of **OsP0P** (Figure S1 in the Supporting Information). This treatment neglects the effect of geometric relaxation on the electronic structure. A large change in the electron density is observed around the central metal atom as expected, indicating that the oxidation process is metal-based. In addition, there is a significant decrease around the polarizable chloride ligand. The electron density associated with the π orbitals of the nitrogen atoms of the bound pyridine groups actually increases, although that associated with the Os−N σ bond decreases. For the carbon atom trans to the bound nitrogen in particular, there is a decrease in the electron density associated with the π orbitals. There is little change in the electron density associated with the unbound pyridine of the P0P ligand, except for a slight increase on the pendent nitrogen.

These results indicate that the electronic properties of the osmium complex on an adsorption surface may be strongly affected by its oxidation state. The fact that the HOMO of **OsP0Pox** is based on the P0P ligand, rather than on the metal

(23) Kober, E. M.; Caspar, J. V.; Sullivan, B. P.; Meyer, T. J. *Inorg. Chem.* **1988**, *27*, 4587−4598.
(24) Kober, E. M.; Marshall, J. L.; Dressick, W. J.; Sullivan, B. P.; Caspar, J. V.; Meyer, T. J. *Inorg. Chem.* **1985**, *24*, 2755−2763.
(25) Guillemoles, J.-F.; Barone, V.; Joubert, L.; Adamo, C. *J. Phys. Chem. A* **2002**, *106*, 11354−11360.
(26) Nazeeruddin, M. K.; Zakeeruddin, S. M.; Kalyanasundaram, K. *J. Phys. Chem.* **1993**, *97*, 9607−9612.

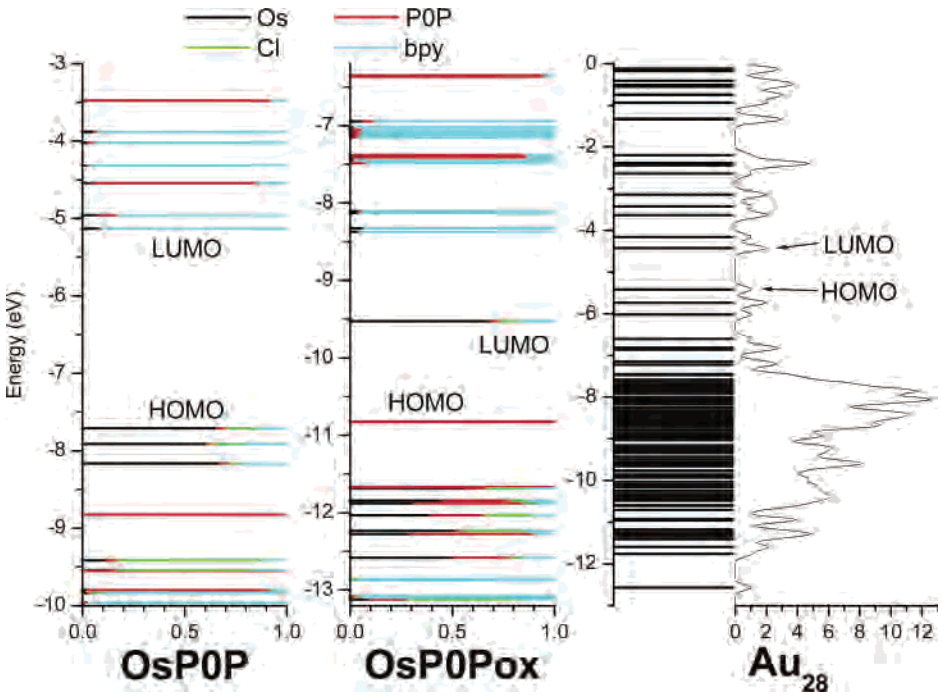

Figure 4. Molecular orbital energies of **OsP0P**, **OsP0Pox**, and Au_{28}. The molecular orbitals of the osmium complexes are described in terms of fractional contributions from the moieties of the molecule. A density of states curve has been convoluted from the molecular orbital data for Au_{28} using Gaussian curves of $w_{1/2}$ of 0.1 eV.

center as for **OsP0P**, means that the coupling between the gold and osmium complexes may be increased in the osmium(III) state compared to the osmium(II) state. This is discussed further below.

Gold Cluster. The gold surface was modeled using a cluster model. Although a cluster model only gives a limited description of the surface band structure, it can be used to investigate local aspects of surface chemistry, including adsorbate−surface interactions.[27] The size of the cluster and basis set used for the Au(111) surface is a tradeoff between speed and accuracy. A realistic description of the chemisorption process requires, at the very least, three layers of atoms, as well as an adequate treatment of the valence electrons of the gold atoms next to the adsorption site.

We used a cluster of 28 gold atoms, arranged into three layers of 13, 12, and 3 atoms (A, B, and C in Figure 2, respectively). All atoms were treated with the small-core LanL2 ECP (60 electrons). The remaining 19 valence electrons were treated with a double-ζ basis set (LanL2DZ) in the case of the central atom of layer A and its immediate neighbors and a minimal basis (LanL2MB) for the remaining atoms. Previous computational studies of adsorption on Au(111) using cluster models have used either a much smaller cluster (Gomes and Illas[28] used a cluster of two layers of 14 and 8 atoms) or a much smaller basis set (Pluchery et al.[29] used a large-core ECP of 78 electrons for all but one of the gold atoms, which means that only one electron was treated explicitly for those gold atoms).

The structure of the gold cluster was optimized under C_{3v} symmetry. This removed most of the strain and allowed the electronic structure of the nanocluster to be represented as accurately as possible within the limitations of the chosen functional and basis set. During the course of the geometry optimization, some movement of the atoms occurred, with the result that neither layer A nor B remained a perfect plane. Although the procedure resulted in a slight dimpling of both of these layers, the overall cluster structure was largely unchanged. This process was followed by monitoring of the pairwise interatomic distances using a histogram. The broadening of the histogram peaks indicated the change from a completely regular lattice to a more disordered structure. In contrast, the cluster studies of Pluchery et al.[29] and Gomes and Illas[28] held the structure of the nanocluster fixed at that of the bulk throughout their calculations. This produces a highly strained nanocluster and ignores surface relaxation effects, which might affect the chemisorption process.

The experimental distance between gold atoms in bulk gold is 2.88 Å.[30] The calculated distance between neighboring atoms in our gold cluster ranges from 2.78 to 3.14 Å, with an average of 2.99 Å. This overestimation is partly due to deficiencies in the DFT functional and basis set but is also due to the low coordination numbers of the atoms, which means that deviation from the results for bulk gold atoms is expected.[31] These results were compared with those of studies of spherical gold clusters of similar size: Wang et al.[32] found

(27) Bagus, P. S.; Illas, F. In *Encyclopedia of Computational Chemistry*; Schleyer, P. V., Allinger, N. L., Clark, T., Gasteiger, J., Kollman, P. A., Schaefer, H. F., III, Schreiner, P. R., Eds.; Wiley: Chichester, U.K., 1998; Vol. 4, p 2870.

(28) (a) Gomes, J. R. B.; Illas, F. *Catal. Lett.* **2001**, *71*, 31−35. (b) Gomes, J. R. B.; Illas, F. *Int. J. Mol. Sci.* **2001**, *2*, 211−220.

(29) Pluchery, O.; Tadjeddine, M.; Flament, J.-P.; Tadjeddine, A. *Phys. Chem. Chem. Phys.* **2001**, *3*, 3343−3350.

(30) *CRC Handbook of Chemistry and Physics*, 64th ed.; Weast, R. C., Ed.; CRC Press: Boca Raton, FL, 1983.

(31) Häberlen, O. D.; Chung, S.-C.; Stener, M.; Rösch, N. *J. Chem. Phys.* **1997**, *106*, 5189−5201.

the average nearest-neighbor distance in Au_{20} to be about 2.80 Å using DFT within the generalized gradient approximation (GGA); Häberlen et al. found a value of 2.86 Å for a 38-atom gold cluster using DFT within the GGA. These studies find shorter average values for the Au−Au distance because they contain fewer surface atoms and, in the case of Wang et al., the cluster studied is the global minimum in energy found after an extensive conformational search.

Figure 4 shows the electronic structure of Au_{28} as a series of energy levels and convoluted as a density of states curve. Bulk metals have a band structure of molecular orbitals. The evolution of this band structure is evident in the occupied portion of the molecular orbitals between about −7.5 and −10 eV, where the density of states curve has a large amplitude. However, a number of discrete energy levels still exist, especially near the frontier region. A gold cluster of 28 atoms is a nanocrystal and has electronic properties different from those of the bulk.[33] Häberlen et al.[31] found that, in general, the HOMO−LUMO gap decreases with increasing cluster size. In bulk gold, the HOMO and LUMO converge to the Fermi level and there is no HOMO−LUMO gap. A HOMO−LUMO gap of 1.0 eV was found for our Au_{28} cluster. This compares with a value of 0.7 eV for the gold cluster of 55 atoms studied by Häberlen et al.[31]

To investigate whether using the larger basis set LanL2DZ for all gold atoms would affect the energies of the frontier occupied orbitals, a single-point energy calculation was carried out at the geometry of the optimized gold cluster using the LanL2DZ basis set and ECP for all atoms. The energies of the 10 highest occupied orbitals (with a range from −5.42 to −7.25 eV) decreased only slightly, with a maximum stabilization of 0.03 eV, indicating that our use of the LanL2MB basis set for 19 of the gold atoms is not too small a basis set to adequately describe the electronic structure of the cluster.

Adsorbed Complexes. The osmium complexes adsorb to the gold cluster through the nitrogen of the pendent pyridine of the P0P ligand. There are a number of possible adsorption sites and orientations for positioning the complex on the surface: the angle of the P0P ligand may be varied with respect to the surface, the dihedral angle between two atoms of the ligand and two atoms of the surface can also be altered, and the nitrogen of the P0P ligand can be positioned over an atom (the "on-top" configuration), over a hollow (between three atoms), or over a bridging site (between two atoms). Pluchery et al.[29] found that the largest adsorption energy for cyanopyridine attached to Au(111) was obtained for the "on-top" position with the C_2 axis of the pyridine ring perpendicular to the surface. Similar results were found by Bilić et al.[34] for pyridine and ammonia. If the C_2 axis of pyridine is perpendicular to the surface, then depending on the dihedral angle between the σ_h plane of the pyridine and two neighboring gold atoms on the surface, there are two possible energy minima: staggered and eclipsed. Bilić et al. found that these had almost the same adsorption energy.

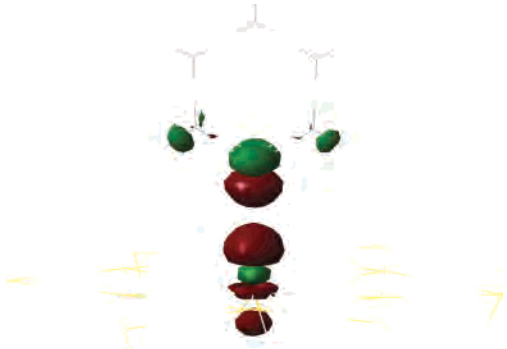

Figure 5. Isosurface of the difference in the electron density between **OsP0P**/Au_{28} and the sum of the electron densities of **OsP0P** and Au_{28} focusing on the interface between the complex and the surface. Green indicates an increase in the electron density, while red indicates a decrease. The isosurface is drawn at 0.004 e bohr^{-3} and is overlaid on a wireframe model of the system for clarity.

In our study, we placed the osmium complex on the surface such that the long axis of the P0P ligand was perpendicular to layer C of the gold cluster and the free nitrogen was directly over the central gold atom of layer A. The initial distance between this gold atom and the nitrogen of the P0P (the distance from 2 to 3 in Figure 2) was set to 2.32 Å for **OsP0P** and 2.58 Å for **OsP0Pox**. The value of 2.32 Å is the optimized distance found by Pluchery et al.[29] for cyanopyridine on Au(111), while 2.58 Å is the optimized distance found for our own Au_{28}/**OsP0P** calculation. The dihedral angle formed by the four atoms 1−4 in Figure 2 was initially set to 0°; this is the staggered conformation.

Because of the detailed treatment of the gold cluster and the size of the osmium complex, the scale of our calculation is much larger than that of previous studies. As a result, the geometry optimization of the adsorbed complexes could only be performed with 2 degrees of freedom. The distance between the complex and the surface, as well as the dihedral angle formed by atoms 1−4 in Figure 2, was optimized for both of the adsorbed complexes **OsP0P** and **OsP0Pox**. The optimized distance between the complex and the surface was 2.58 Å for **OsP0P** and 2.54 Å for **OsP0Pox**, while the dihedral angle remained close to zero in each case (0.0° for **OsP0P** and 0.6° for **OsP0Pox**), keeping the complex in the staggered conformation. These results agree well with those of Bilić et al.[34] for the absorption of pyridine on Au(111) (equilibrium bond length of 2.46 Å) and of Pluchery et al.[29] for the binding of cyanopyridine to Au(111) (equilibrium bond length of 2.32 Å).

Figure 5 shows the change in the electron density associated with the adsorption of **OsP0P** on the gold surface. This diagram was created by summing the electron densities of the complex and the surface, which were calculated separately at their geometry in the adsorbed system, and then subtracting the electron density of the adsorbed system. The electron density has decreased in the area between the adsorbed nitrogen and the central gold atom. There is a corresponding increase in the electron density on the nitrogen

(32) Wang, J.; Wang, G.; Zhao, J. *Phys. Rev. B* **2002**, *66*, 035418.
(33) Rao, C. N. R.; Kulkarni, G. U.; Thomas, P. J.; Edwards, P. P. *Chem.—Eur. J.* **2002**, *8*, 29−35.
(34) Bilić, A.; Reimers, J. R.; Hush, N. S. *J. Phys. Chem. B* **2002**, *106*, 6740−6747.

and on the gold atom. Bilić et al.[34] created similar diagrams for the adsorption of pyridine and ammonia on Au(111). They noted that the change in the electron density is small. In regards to the bonding interaction, they noted that there is no evidence for covalent bonding effects because the electron density *decreases* in the area between the adsorbate and the surface. The major effect appears to be internal charge redistribution, or polarization, rather than charge transfer.

A comparison of the energy levels of the gold cluster before and after adsorption (Figure S4 in the Supporting Information) shows a shift to lower energy of about 0.85 eV in Au_{28}/**OsP0P**. A much smaller shift to lower energy is observed for the energy levels of the osmium complexes: about 0.05 eV for **OsP0P**. However, some of the energy levels have shifted more than 0.05 eV, and others have mixed with energy levels from the gold. Indeed, the HOMO−3 seems to disappear completely upon adsorption. This orbital is almost completely P0P-based (Figure 4) and so is expected to interact strongly with the gold surface. These results are not unexpected and are in line with experimental observations. For the type of osmium complexes investigated here, surface redox potentials are usually close to the solution value,[19,35] and comparisons between surface-enhanced Raman and solution-based resonance Raman data show that shifts in the vibrational frequencies of the ligands close to the metal ion are usually small.[36] The effect of adsorption is not so strong that the complex loses its electronic identity on the surface.

To investigate this further, a series of single-point energy calculations were performed for several values of the Au_{28}−**OsP0P** distance, from the optimized distance of 2.58 Å to 6.18 Å. Figure 6 shows the resulting energy levels for four different Au−N values. At a distance of 6.18 Å, there is no mixing between the orbitals of the gold cluster and the complex. The HOMO−3 from the isolated **OsP0P** is marked with an asterisk (*) in Figure 6. As the molecule is moved closer to the surface, the HOMO−3 starts to split and mix with the gold energy levels, until there is no trace of it at the original energy.

The adsorption energy, E_{ads}, for Au_{28}/**OsP0P** was calculated using the following formula:

$$E_{ads} = E(Au_{28}) + E(\textbf{OsP0P}) - E(Au_{28}/\textbf{OsP0P})$$

where $E(Au_{28}/\textbf{OsP0P})$ indicates the energy of the system shown in Figure 2 and was found to be 9.2 kcal mol^{-1}. After correction for basis set superposition error (BSSE) (2.5 kcal mol^{-1}) and the loss of translational and rotational entropy of the **OsP0P** upon adsorption (1.8 kcal mol^{-1}), this is reduced to 6.7 kcal mol^{-1}. This is close to the value found by Bilić et al.[34] for the absorption energy of pyridine on Au(111), 7.3 kcal mol^{-1}, although considerably less than that found by Pluchery et al.[29] for cyanopyridine on Au(111),

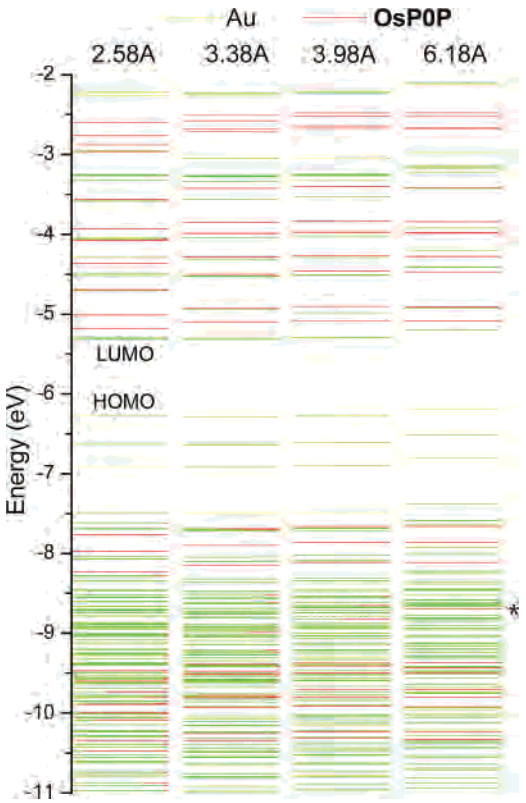

Figure 6. Effect of an increase in the Au−N distance on the energy levels of Au_{28}/**OsP0P**. The Au−N distance is given in angstroms above each graph. Energy levels to which **OsP0P** contributes are indicated by red, while green is used for energy levels involving the gold cluster. The red energy level, marked with an asterisk (*) at 6.18 Å, is the HOMO−3 of isolated **OsP0P**.

33.5 kcal mol^{-1}. The accuracy of such adsorption energy values is limited because their magnitudes are small compared to the total energy of the system. Nevertheless, our result is in good agreement with the experimental results for the structurally related osmium complexes $[Os(bpy)_2(P3P)Cl]^+$ and $[Os(bpy)_2(P3P)_2]^{2+}$ (where P3P is 4,4′-dimethylenedipyridine), which have free energies of adsorption of 9.1 and 7.1 kcal mol^{-1}, respectively.[37]

A similar calculation for Au_{28}/**OsP0Pox** indicated that **OsP0Pox** adsorbs much more strongly, having an adsorption energy of 38.7 kcal mol^{-1} (34.4 kcal mol^{-1}, assuming a BSSE of 2.5 kcal mol^{-1} and correcting for the loss of entropy upon adsorption). However, visualization of the spin density in the adsorbed species shows that the unpaired electron is actually based on the gold cluster, suggesting that the system is more correctly viewed as Au_{28}ox/**OsP0P**; that is, the gold cluster is more easily oxidized than the osmium complex. A comparison of the energy levels of the adsorbed species with those of Au_{28}ox and **OsP0P** shows that this is indeed the case (Figure S5 in the Supporting Information). The calculated absorption energy for Au_{28}ox/**OsP0P** is, in fact, negative, at −9.5 kcal mol^{-1} (−13.8 kcal mol^{-1}, assuming a BSSE of 2.5 kcal mol^{-1} and correcting for the loss of entropy upon adsorption). This highlights a limitation of the use of a cluster model to represent the adsorption of an oxidized complex to a surface; the oxidation potential of the

(35) Forster, R. J.; Loughman, P.; Keyes, T. E. *J. Am. Chem. Soc.* **2000**, *122*, 11948−11955.
(36) Farquharson, S.; Weaver, M. J.; Lay, P. A.; Magnuson, R. H.; Taube, H. *J. Am. Chem. Soc.* **1983**, *105*, 3350−3351.
(37) Forster, R. J.; O'Kelly, J. P. *J. Electrochem. Soc.* **2001**, *148*, E31−E37.

bulk metal can be quite different from that of a nanocluster, thus making it difficult to obtain results that are representative of the bulk.

Because of the size of the system studied here, it was not possible to take into account the effect of the solvent. Although inclusion of the solvent is not expected to significantly affect the geometry of the complex,[25] it will affect the energies and composition of the molecular orbitals, as well as the adsorption energy. In a study of the solvatochromism of *cis*-[Ru(4,4′-COOH-2,2′-bpy)$_2$(NCS)$_2$], Fantacci et al.[38] found that calculations including water as the solvent resulted in an increase of the HOMO−LUMO gap from 0.50 eV in the gas phase to 1.24 eV in water. When the solvent was included, the frontier occupied orbitals had greater contributions from the metal center because of a larger stabilization of orbitals involving the thiocyanate ligands. Adsorption energetics may also be strongly affected by neglect of the solvent, as shown in a study by De Angelis et al.,[39] where the most stable binding mode, monodentate or bidentate, of $[Fe(CN)_6]^{4-}$ on a TiO_2 cluster model, depended on whether the calculation was carried out in a vacuum or in water.

Conclusions

As components in molecular devices, osmium polypyridyl complexes possess a number of desirable features. They are stable and redox-active and have tunable photophysical and electrochemical properties. For practical molecular devices, where surfaces form the necessary connection to the macromolecular world, it is vital to understand the electronic changes that occur upon adsorption to the surface. We have carried out the first DFT calculations of an osmium complex attached to a gold surface. This study shows that DFT is a very useful tool in this regard especially where oxidation of the molecule is an important part of the operation of the device. The model obtained is realistic, and this approach can be used to predict the behavior of other similar compounds. A number of observations can be made.

Partial optimization of the cluster, combined with a full optimization of the complex, needs to be performed prior to investigation of the electronic levels of the adsorbed complex. Importantly, oxidation of the osmium complexes involves a considerable reordering of the energy levels of the complex. The HOMO changes from being metal-based to being based on the P0P ligand, specifically on the pendent pyridine ring of P0P. The results obtained further indicate that the interaction between the surface and the complex does not involve covalent bonding but rather involves polarization at the adsorbate/substrate interface. Apart from a general shift in energy, the orbitals of the complex and the gold surface are not perturbed to a significant extent by the adsorption process, except for those orbitals based on the P0P ligand. The size of the gold cluster employed, although adequate to describe the bonding interaction in Au_{28}/**OsP0P**, was found to reproduce the electronic structure of a nanocluster rather than bulk gold. As a result, oxidation of the adsorbed complex removed an electron from the nanocluster rather than the adsorbed osmium complex, as is observed experimentally. This appears to be a limitation of the use of cluster models in the study of adsorbed oxidized species.

This study alone is not sufficient to allow us to fully investigate several aspects of importance to molecular electronics. The delocalization of the molecular energy levels such as the P0P-based HOMO−3 over the gold surface should lead to a lower contact resistance and would suggest that the conduction path involves such delocalized orbitals rather than the HOMO and LUMO. To keep the system at a tractable size, solvent and counterion effects, which are expected to influence the energetics of the adsorption process, have been omitted. We are continuing further studies that will address these issues in greater detail.

Acknowledgment. This work was partly supported by EU FP6 through the SUSANA network (HPRN 2001-0085). N.M.O'B. thanks Enterprise Ireland for funding and A. Coghlan for her helpful comments.

Supporting Information Available: Partial density of states spectra for **OsP0P** and **OsP0Pox**, along with molecular orbital information in table format, a figure showing the instantaneous change in the electron density upon oxidation of **OsP0P**, a comparison of the energy levels of Au_{28}/**OsP0P** with those of Au_{28} and **OsP0P**, and a comparison of the energy levels of Au_{28}ox/**OsP0P** with those of Au_{28}ox and **OsP0P**. This material is available free of charge via the Internet at http://pubs.acs.org.

IC060903E

(38) Fantacci, S.; De Angelis, F.; Selloni, A. *J. Am. Chem. Soc.* **2003**, *125*, 4381−4387.
(39) De Angelis, F.; Tilocca, A.; Selloni, A. *J. Am. Chem. Soc.* **2004**, *126*, 15024−15025.